Dependence of the Forward-Backward Asymmetry in $t\bar{t}$ Production on the $M_{t\bar{t}}$ Invariant Mass

The CDF Collaboration

URL http://www-cdf.fnal.gov/cdfnotes/cdf9853_Afb_Mtt.pdf

(Dated: July 20, 2009)

The Collider Detector at Fermilab has observed a forward-backward asymmetry in $t\bar{t}$ production of $A_{FB} = 0.193 \pm 0.069_{stat+syst}$ in 3.2 fb^{-1}. In this paper we present a measurement of the A_{FB} dependence on the invariant mass $M_{t\bar{t}}$ of the $t\bar{t}$ system in the same dataset. A sample of 776 events characterized by one leptonic top decay plus four or more jets, one of which is b-tagged, are reconstructed with a χ^2 fit to the $t\bar{t}$ kinematic hypothesis. Using an unfolding technique, we unsmear the effects of the reconstruction back to parton level simultaneously in the rapidity and $t\bar{t}$ invariant mass variables. The result is presented as a scan of the forward-backward asymmetry in the $p\bar{p}$ frame for the semi-inclusive samples below and above eight different $M_{t\bar{t}}$ thresholds.

Preliminary Results for Summer 2009 Conferences

I. INTRODUCTION

This note reports on the measurement of the dependence of the forward-backward asymmetry A_{FB} observed in top pair events identified with the CDF detector at Fermilab [1] on the invariant mass $M_{t\bar{t}}$ of the $t\bar{t}$ system. In a sample of 3.2 fb^{-1}, CDF observes an imbalance in the number of top quarks produced at parton level along the direction of the incoming proton vs the direction of the anti-proton equal to $A_{FB} = 0.193 \pm 0.065(\text{stat}) \pm 0.023(\text{syst})$ [2]. This is to be compared to the NLO prediction of the $p\bar{p}$ frame asymmetry $A_{FB} = 0.05 \pm 0.015$ [5]. The D0 Collaboration measures $A_{FB} = 0.12 \pm 0.08$ at the reconstruction level [4].

A possible interpretation of the excess observed in the data is the presence of extra particles decaying to $t\bar{t}$ with a large forward-backward asymmetry [5]. Direct searches for evidence in the $M_{t\bar{t}}$ spectrum of a Z'-like narrow resonance or a new massive color-octet particle interfering with the standard gluon octet, have been already performed in CDF without any positive results [6–8]. The dependence of A_{FB} on $M_{t\bar{t}}$ is another natural way to look for a new top pair production channel.

The kinematics of the top and anti-top decays are reconstructed using the same χ^2-based fitter used to measure the top mass. This mass fitter has a resolution with long non-gaussian tails, especially in $M_{t\bar{t}}$. Hence the need to unfold the effects of the mass fitter reconstruction back to the original $t\bar{t}$ decay in the $p\bar{p}$ frame, not only for the angle of the t ($\bar{t}$) quark w.r.t. the incoming p ($\bar{p}$) but also for the overall kinematics of the event used in the invariant mass measurement. To keep into account the correlation between the angle, measured via the rapidity of the hadronically decaying top quark, and the invariant mass, we employ a two variable unfolding technique simultaneously in y_{had} and $\mathcal{M}_{t\bar{t}}$ [10] We use four bins in the unfolding procedure: a forward rapidity and a backward rapidity bin for each of the invariant mass regions above and below a predetermined threshold. To avoid possible biases due to an arbitrary choice of $M_{t\bar{t}}$ threshold, we scan A_{FB} across eight different values of $t\bar{t}$ invariant mass ranging from 400 to 800 GeV/c^2. Using the number of events returned by the unfolding, we measure semi-integral A_{FB} as a function of $M_{t\bar{t}}$ at the parton level.

Section II reports on the data sample and Monte Carlo simulation samples used in the analysis. In Section III we review the definition of A_{FB} and how we measure it using reconstructed variables. A generic $M_{t\bar{t}}$ dependent forward-backward asymmetry model implemented for our unfolding performance studies and based on a Next-to-Leading (NLO) calculation, is presented in Section IV. Section V reports on the checks of our measurement methodology. Section VI contains the results for A_{FB} scan vs $M_{t\bar{t}}$ in our data. Section VII summarizes the findings of this analysis.

II. DATA SAMPLE & EVENT SELECTION

For this measurement we analyse the 3.2 fb^{-1} data sample used to measuring the integral forward-backward asymmetry at parton level of $A_{FB} = 19.3 \pm 6.9_{\text{stat+sys}}$ in the $p\bar{p}$ frame [2]. The sample has 776 events with one high P_T lepton (CEM, CMUP or CMX), $\not{E}_T > 20$ GeV and 4 or more Tight Jets, of which at least 1 has a SecVTX tag. An anti-tag sample of 1728 events passing the same selection criteria but with no SecVtx tags is used to validate our background model. The background is calculated using a combination of Monte Carlo samples and data samples. For details of the event selection and background models used, see [2].

Figure 1 compares the observed rapidity and top-antitop invariant mass distributions in data to the expectations for $t\bar{t}$ Pythia MC plus background. The Pythia MC used throughout this analysis to model the production and decays of $t\bar{t}$ events at $\sqrt{(s)} = 1.96$ TeV is based on a leading order generator with null forward-backward asymmetry. Figure 2 shows the top-antitop invariant mass distribution, separately for events reconstructed as forward (FW), that is with positive rapidity, vs backward (BW) or with negative rapidity. Both distributions start at the kinematically allowed threshold of about 350 GeV/c^2 and decreases very rapidly as expected for the almost threshold production of top pairs at the Tevatron energies. The choice of equispaced $\mathcal{M}_{t\bar{t}}$ edges between 400 GeV/c^2 and 800 GeV/c^2 has the advantage of scanning the full physically allowed spectrum at intervals comparable to our mass resolution but suffers from very low statistics in the high mass region passed the 500 GeV/c^2 $\mathcal{M}_{t\bar{t}}$ threshold.

Figure 3 compares the rapidity of the hadronically decaying top observed in data to the expectations for signal events, for which the signal to background ratio is predicted to be S:(S+B) = 3:1, and for background events, for which S:(S+B) = 1:5. For both samples, we divide the events in "low" mass and "high" mass events with respect to a reconstructed $\mathcal{M}_{t\bar{t}}$ threshold of 450 GeV/c^2.
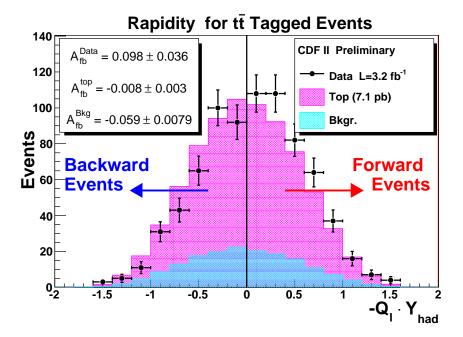
Rapidity for t̄t Tagged Events

$A_{fb}^{Data} = 0.098 \pm 0.036$

$A_{fb}^{top} = -0.008 \pm 0.003$

$A_{fb}^{Bkg} = -0.059 \pm 0.0079$

Backward Events

Forward Events

CDF II Preliminary

Data L=3.2 fb^{-1}

Top (7.1 pb)

Bkgr.

Events

$-Q_l \cdot Y_{had}$

FIG. 1: Reconstructed rapidity distribution y_{had}, multiplied by the opposite of the charge of the lepton in the event Q_ℓ, for ≥4 Tight jets events with at least one b-tag. Data (points) are superimposed to the sum of top Pythia MC (pink histogram) and background (light blue histogram). The legend to the right of each plot gives the raw asymmetries for each of the three contributions. Events are divided in BW vs FW as the y_{had} crosses the null value.
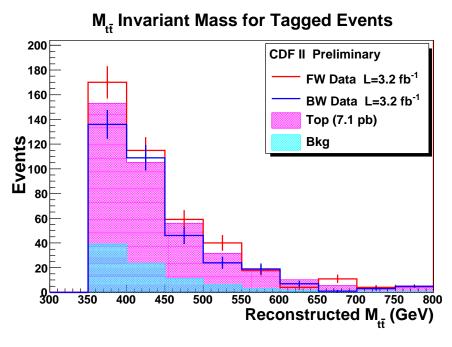
M$_{t\bar{t}}$ Invariant Mass for Tagged Events

CDF II Preliminary

FW Data L=3.2 fb^{-1}

BW Data L=3.2 fb^{-1}

Top (7.1 pb)

Bkg

Events

Reconstructed M$_{t\bar{t}}$ (GeV)

FIG. 2: Reconstructed t̄t invariant mass $\mathcal{M}_{t\bar{t}}$ for FW vs BW events with ≥4 Tight jets and at least one b-tag. Data (points) are superimposed to the sum of top Pythia MC (pink histogram) and background (light blue histogram). For simplicity, the MC predictions are normalized to half of the predicted value for a sample of 3.2 fb^{-1} integrated luminosity.
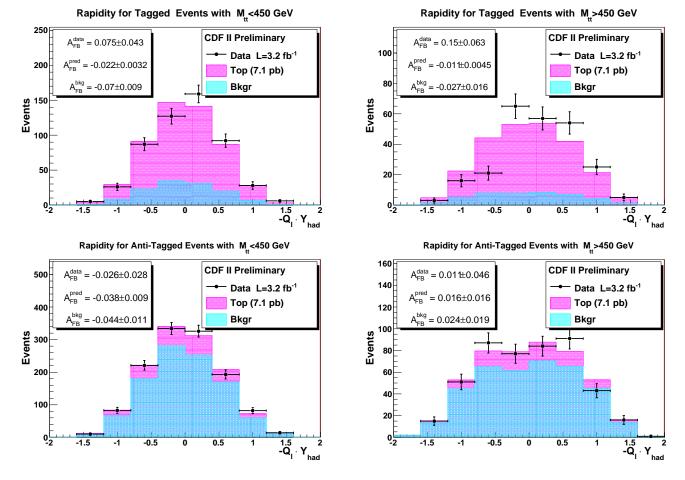
FIG. 3: Reconstructed rapidity distribution y_{had}, multiplied by the opposite of the charge of the lepton in the event Q_ℓ, for ≥ 4 Tight jets events with at least one b-tag (top plots) and no b-tags (bottom plots). Data (points) are superimposed to the sum of top Pythia MC (pink histogram) and background (light blue histogram). The legend to the right of each plot gives the raw asymmetries for each of the three contributions. The plots on the left and on the right are for events with $\mathcal{M}_{t\bar{t}} < 450$ GeV/c^2 and $\mathcal{M}_{t\bar{t}} > 450$ GeV/c^2, respectively.

III.   FORWARD-BACKWARD ASYMMETRY OVERVIEW

In the p$\bar{\text{p}}$ frame, the integral forward-backward asymmetry at parton level is defined as:

$$A_{\text{FB}} = \frac{N_t(Y > 0) - N_t(Y < 0)}{N_t(Y > 0) + N_t(Y < 0)} \tag{1}$$

The rapidity Y is the natural choice of angular variable in inclusively measured hadron interactions. Assuming CP invariance, $N_t(Y < 0) = N_{\bar{t}}(Y > 0)$ and the A_{FB} asymmetry is equivalent to the t$\bar{\text{t}}$ production charge asymmetry [3].

From distributions like in Figure 3, we can measure the "low" and "high" mass region raw asymmetries $\mathcal{A}_{\text{FB}}$ defined as:

$$\mathcal{A}_{\text{FB}}^{\text{i}} = \frac{N_t^{\text{i}}(-Q_\ell \cdot y_{\text{had}} > 0) - N_t^{\text{i}}(-Q_\ell \cdot y_{\text{had}} < 0)}{N_t^{\text{i}}(-Q_\ell \cdot y_{\text{had}} > 0) + N_t^{\text{i}}(-Q_\ell \cdot y_{\text{had}} < 0)} \tag{2}$$

where y_{had} is the reconstructed rapidity of the hadronically decaying top multiplied by the opposite of the charge of the leptonically decaying top, Q_ℓ. The subscript "i" stands for the the two separate "low" and "high" mass regions.

The rapidity of the hadronically reconstructed top quark is chosen because it measured more precisely than the rapidity of the leptonically decaying top quark, which is confounded by the missing energy and neutrino z-direction.

The lepton charge Q_ℓ identifies the flavour of the hadronically decaying top quark and by using the product $-Q_\ell \cdot Y_{had}$ we effectively combine the $t(\bar{t})$ angle along the $p(\bar{p})$ direction into a single distribution, which is valid if the system has CP invariance.

In order to go from the raw $\mathcal{A}_{FB}$ in $p\bar{p}$ frame to the true parton level A_{FB} in the $p\bar{p}$ frame as in equation 1, the measured asymmetry is corrected for the dilution introduced by the mass fitter solution and bias due to the selection of $t\bar{t}$ events. In this analysis of A_{FB} vs. $M_{t\bar{t}}$, we also confront the smearing of the $M_{t\bar{t}}$ distribution, simultaneously unfolding both A_{FB} and $M_{t\bar{t}}$ to the parton level values.

The formalism used for this correction can be summarized as:

$$\vec{N}_{cor} = (A^{-1} \cdot S^{-1}) \, \vec{N}_{bkg-sub} \tag{3}$$

where $\vec{N}_{bkg-sub}$ is a four dimensional vector in the two variable event space of top rapidity by top-antitop invariant mass after subtracting the background contamination. More explicitly, $\vec{N} = (FW_{low}, BW_{low}, FW_{high}, BW_{high})$ where the subscripts "low" and "high" stand for events in mass regions below and above the threshold. The two 4×4 inverted matrices S^{-1} and A^{-1} are calculated using the $M_t = 175 \text{ GeV}/c^2$ Pythia Monte Carlo. They take care of unfolding the effects of the reconstruction and $t\bar{t}$ selection, respectively, simultaneously for the Y and $M_{t\bar{t}}$ variables. More explicitly, the matrix A is diagonal and each term a_{ii} gives the fraction of true $t\bar{t}$ events passing the l+jet+SECVTX selection. The smearing matrix S has components s_{ij} calculated as the fraction of selected events in the true j-th bin found in reconstructed i-th bin. The vector $\vec{N}_{cor}$ contains the corrected number of events used inside equation 1 to calculate the final forward-backward asymmetry in the $p\bar{p}$ frame, A_{FB}, independently for the "low" and "high" mass region, defined now with respect to the truth $M_{t\bar{t}}$ invariant mass. For our final result, we repeat the unfold for different values of the invariant mass threshold and present our final result as a semi-integral A_{FB} over 8 different $M_{t\bar{t}}$ edges ranging from 400 to 800 GeV/c^2.

IV.   MODEL OF $M_{t\bar{t}}$ DEPENDENT A_{FB}

As a generic model of A_{FB} dependence on $M_{t\bar{t}}$, used for producing templates of known asymmetry and study the performance of our unfolding technique, we use the predictions of a recent theoretical calculation of the NLO QCD charge asymmetry [9]. This paper uses resummation techniques to address the issue of NNLO corrections and find them to be small. Figure 4 shows a plot of $A_{FB}^{t\bar{t}}$ vs $M_{t\bar{t}}$ from this paper, with results from different resummation calculation in black solid and dashed line. This is the mass dependence in the $q\bar{q}$ frame, including the effects of PDFs. For our study we will assume this is reasonably approximated by the $t\bar{t}$ frame. The overall suggestion is a linear dependence of the forward-backward asymmetry on the top pair invariant mass. The green solid line shows an approximate fit of the resummed predictions which we parametrize as:

$$A_{FB} = A_{FB}^0 + (\Delta A_{FB}/\Delta M_{t\bar{t}}) \cdot (M_{t\bar{t}} - 350) \tag{4}$$

where the offset $A_{FB}^0 = 0.03$ is the asymmetry value at the $t\bar{t}$ threshold value of of 350 GeV/c^2 and the slope $\Delta A_{FB}/\Delta M_{t\bar{t}} = 0.025$ is in units of $(100 \text{ GeV}/c^2)^{-1}$. In summary, the NLO model predicts a forward-backward asymmetry in the $t\bar{t}$ frame starting at 3% and increasing by 2.5% every 100 GeV/c^2 interval above 350 GeV/c^2.

V.   UNFOLD TESTS

In order to understand the precision and predictability of our measurement, we input control samples with known asymmetry to the two variable unfolding machinery and compare the result for the corrected A_{FB} to the input value A_{FB}^{IN}. Our control samples, also referred to as templates, are generated starting from a $M_t = 174 \text{ GeV}/c^2$ Pythia $t\bar{t}$ sample by reweighting the top angular distribution in the $t\bar{t}$ frame according to the following "ansatz": we assume that the differential cross section $d(\sigma)/d\cos\theta_{t\bar{t}}$ have, on top of the standard model component $K \cdot (1 + \cos\theta_{t\bar{t}}^2)$, an extra asymmetric $A_{FB} \cdot \cos\theta_{t\bar{t}}$ component, modulated by an amplitude $A_{FB} = A_{FB}(M_{t\bar{t}})$ linearly dependent on the $t\bar{t}$ mass. This "ansatz" is closely modelled on the known physics example of forward-backward asymmetry for the Z-boson and we will be often referred to as the $A_{FB} \cdot \cos\theta$ model. The mass dependent asymmetry in the $t\bar{t}$ frame for this model is of the form:

$$A_{FB}(M_{t\bar{t}}) = A_{FB}^0(M_{t\bar{t}}^0) + dA_{FB}/dM_{t\bar{t}} \times (M_{t\bar{t}} - M_{t\bar{t}}^0). \tag{5}$$

where $M_{t\bar{t}}^0 = 350 \text{ GeV}/c^2$, which is inspired by the linear fit to the calculation of Sterman et al. [9] of Section IV.
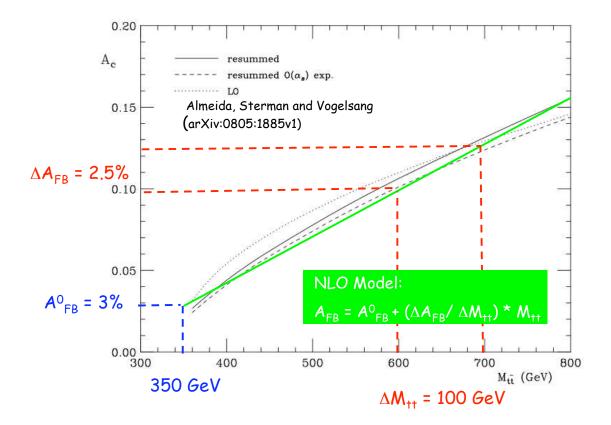
FIG. 4: Predicted forward-backward asymmetry in $t\bar{t}$ production vs the top-antitop invariant mass at the Tevatron energies. The black solid and dashed line come from two different resummation calculations of the NLO prediction (dotted line). The green solid line is a linear fit of the resummation predictions, parametrized as $\mathrm{A_{FB}} = \mathrm{A_{FB}^0} + (\Delta \mathrm{A_{FB}}/\Delta \mathrm{M_{t\bar{t}}}) \cdot (\mathrm{M_{t\bar{t}}} - 350)$, with $\Delta \mathrm{A_{FB}}/\Delta \mathrm{M_{t\bar{t}}} = 2.5\%$ is in units of asymmetry change every $100~\mathrm{GeV}/c^2$ and $\mathrm{A_{FB}^0} = 3\%$ is the initial asymmetry for events at the $\mathrm{M_{t\bar{t}}} = 350\mathrm{GeV}/c^2$ kinematic threshold.

The practical implementation of different $\mathrm{A_{FB}^{IN}} \cdot \cos\theta$ templates to be used in the two variable unfolding is not done using an event-by-event reweight but rather by rescaling the contents of 2D histograms of rapidity and invariant mass for the $\mathrm{M_t} = 174\mathrm{GeV}/c^2$ Pythia MC sample. These 2D histograms preserve the correlation between the rapidity and invariant mass distributions of top quarks across different reference frames ($t\bar{t}$ vs $p\bar{p}$) or different analysis levels (truth vs reconstruction). We choose a total number of 160 bins, 10 bins in invariant mass, and 16 bins in rapidity, for each axis.

We tested for possible biases of two variable unfolding technique by comparing the corrected $\mathrm{A_{FB}}$ returned by the unfold to the truth asymmetry for templates generated with a given choice of input $(\mathrm{A_{FB}^0}, \mathrm{dA_{FB}/dM_{t\bar{t}}})$ spanning the allowed physical region of $\mathrm{A_{FB}(M_{t\bar{t}})}$ between -100% and 100%.

We factorize these studies by varying one parameter at the time, that is we compare unfolded vs truth asymmetries for a null offset $\mathrm{A_{FB}^0} = 0$ and slope $\mathrm{dA_{FB}/dM_{t\bar{t}}}$ changing from -10% to +10% $(100~\mathrm{GeV}/c^2)^{-1}$ in 1% steps in one case and for a null slope but constant $\mathrm{A_{FB}^0}$ changing from -100% to +100% in 10% steps in the other. The general conclusion from these studies is that there is some bias in the two variable unfolding method, with a tendency for the corrected asymmetry to overestimate the truth input value. The bias becomes more severe when the low vs high

mass threshold moves toward high $M_{t\bar{t}}$ values, as expected given the rapidly diminishing event statistics in the high mass region. Nevertheless, the bias is always smaller than the statistical uncertainty of our measurement and we will add it to the systematic uncertainty of our result, as discussed in the next section.

VI. RESULTS

In sections III and V we laid down the method used to measure a mass dependent parton level forward-backward asymmetry using a simultaneous unfolding of the rapidity and invariant mass variables and demonstrated that we can reliably measure asymmetries over a large range of $M_{t\bar{t}}$ threshold values.

On the way to measure A_{FB}^{low} and A_{FB}^{high} in the data over the full $M_{t\bar{t}}$ spectrum, we first present presents the details for the below and above asymmetry for a particular choice of mass threshold, namely $M_{t\bar{t}} = 450$ GeV/c^2.

The number of data events before background subtractions is $\vec{N}_{raw} = (FW_{low}, BW_{low}, FW_{high}, BW_{high}) = (285,245,141,105)$, which results in the raw asymmetry presented in Table I. The background itself has a negative asymmetry centered around -6% with a slight mass dependence. After background subtraction $\vec{N}_{bkg-sub} == (229, 181, 118, 80)$. The acceptance matrix A and unsmearing matrix S, calculated using the standard Pythia $M_t = 175$ GeV/c^2 Monte Carlo, are as following:

$$A = \begin{bmatrix} 0.915 \pm 0.004 & 0 \pm 0 & 0 \pm 0 & 0 \pm 0 \\ 0 \pm 0 & 0.956 \pm 0.004 & 0 \pm 0 & 0 \pm 0 \\ 0 \pm 0 & 0 \pm 0 & 1.06 \pm 0.01 & 0 \pm 0 \\ 0 \pm 0 & 0 \pm 0 & 0 \pm 0 & 1.15 \pm 0.01 \end{bmatrix} \quad (6)$$

$$S = \begin{bmatrix} 0.760 \pm 0.004 & 0.119 \pm 0.002 & 0.274 \pm 0.003 & 0.085 \pm 0.002 \\ 0.113 \pm 0.002 & 0.748 \pm 0.004 & 0.073 \pm 0.001 & 0.282 \pm 0.003 \\ 0.108 \pm 0.002 & 0.023 \pm 0.001 & 0.613 \pm 0.004 & 0.048 \pm 0.001 \\ 0.019 \pm 0.001 & 0.109 \pm 0.002 & 0.040 \pm 0.001 & 0.586 \pm 0.004 \end{bmatrix} \quad (7)$$

Fig. 5 shows the results of the unfold on 3.2 fb^{-1} of top pair reconstructed data: for the below mass region, the semi-integral raw asymmetry after background subtraction of $\mathcal{A}_{FB}^{low} = 11.8 \pm 5.6\%$ gets corrected by the unfold to $A_{FB}^{low} = 16.4 \pm 10.3\%$ at parton level while the above mass region sees the raw value of $\mathcal{A}_{FB}^{high} = 18.9 \pm 7.8\%$ gets corrected to $A_{FB}^{high} = 25.7 \pm 12.7\%$.

Fig. 6 shows the result for the semi-integral A_{FB} below and above different $M_{t\bar{t}}$ thresholds for eight parton level mass edges ranging between 400 GeV/c^2 and 800 GeV/c^2. Details on the numeric value of the asymmetries at each step of the unfolding procedure are presented in Table I. Each point in Fig. 6 has two sets of error bars: the inner ones correspond to the statistical uncertainty and the outer ones to the sum in quadrature of the statistical and systematics uncertainties, as reported in the last columns of Table I. We consider three different sources of systematic uncertainties: systematics from the background model, systematics from the top signal model and systematics from the unfolding procedure. Each systematics is derived by comparing the unfolded value for a template model of integral asymmetry consistent with was measured in the data to the unfolded result for a "systematic" model with either modified shape or background components. As our templates of known asymmetries are characterized by the two parameters, $(A_{FB}^0, dA_{FB}/dM_{t\bar{t}})$, as discussed in Section IV, we considered all of templates with integral asymmetry consistent with $A_{FB} = 19.3 \pm 6.5\%$ when comparing to the systematic model and chose to quote as systematics uncertainty the comparison with the largest difference.

The systematic uncertainty on the background has two components, one coming from the uncertainty on the background overall normalization and one coming from the uncertainty on the background shape. They make up for the single largest systematics contribution for asymmetries in mass regions with large number of events and the second largest contribution, after the unfolding systematics, for mass regions with limited data statistics. The systematics due to the signal models have contributions from the modelling of initial and final state radiation, jet energy scale, parton distribution functions and different Monte Carlo $t\bar{t}$ simulations. Overall, they tend to represent the smallest contributions to the total systematic uncertainty. Finally, the systematics due to the unfolding technique sum together the effects of biases in the correction procedure, already discussed in Section V, and the effect of a different model for producing a non null asymmetry coming from comparing Pythia vs a NLO simulation generated with the MC@NLO matrix element calculation. Their sum tends to be the single largest contribution to the systematic uncertainties in mass regions with a limited statistics.

Figures 6 compares the results of the unfolding in the data to two predictions, one coming from an asymmetric model with flat mass dependence for its input A_{FB} (dashed line) and one from an asymmetric model with some mass
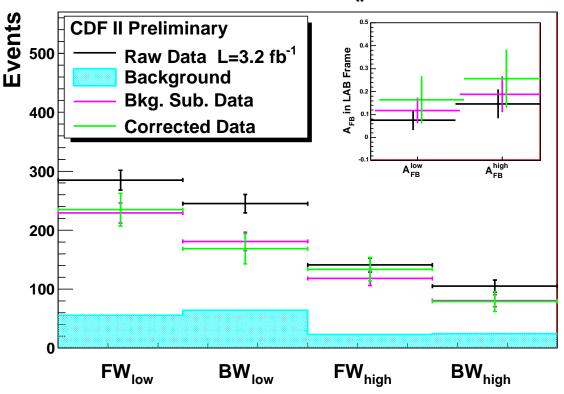
FIG. 5: Number of data events in the four mutually exclusive bins, ($FW_{Low}, BW_{Low}, FW_{High}, BW_{High}$), used for two variable unfolding measurement of A_{FB} vs $M_{t\bar{t}}$. A cut on $M_{t\bar{t}}$ at 450 GeV/c^2 separate the below from the above regions. Shown are the original number of raw data events (black line), the background contribution (light blue fill), the background subtracted number of events (pink line) and the final corrected number of events (green line) after the unfolding. The inset at the top right corner shows the corresponding asymmetries at different stages of the unfolding procedure.

dependence (green line). The first is calculated using a template of null $dA_{FB}/dM_{t\bar{t}}$ and A^0_{FB} such to generate an integral $A_{FB} = 19.3\%$, as measured in the data. The second model assumes $dA_{FB}/dM_{t\bar{t}} = 2.5\%$ and $A^0_{FB} = 3\%$ as derived from the fit to the NLO calculation.

VII. CONCLUSIONS

We present an analysis of the top forward-backward asymmetry dependence on $M_{t\bar{t}}$ for a data sample corresponding to an integrated luminosity of 3.2 fb^{-1}. The sample is selected by requiring one high p_T lepton, either electron or muon, one neutrino and at least 4 jets, one of which is tagged by the presence of a jet consistent with a b-hadron decay. Using a two variable unfolding in rapidty and top-antiop invariant mass, we measure the semi-integral forward-backward asymmetries in low and high $M_{t\bar{t}}$ regions defined with respect to eight different $M_{t\bar{t}}$ threshold values ranging from 400 to 800 GeV/c^2. Our results are compared to two models, one with $M_{t\bar{t}}$ independent integral $A_{FB} = 19.3\%$ and one with a A_{FB} linearly dependent on the invariant mass of the $t\bar{t}$ system and consistent with a recent NLO calculation.

[1] F. Abe, et al., Nucl. Instrum. Methods Phys. Res. A **271**, 387 (1988); D. Amidei, et al., Nucl. Instum. Methods Phys. Res. A **350**, 73 (1994); F. Abe, et al., Phys. Rev. D **52**, 4784 (1995); P. Azzi, et al., Nucl. Instrum. Methods Phys. Res. A **360**, 137 (1995); The CDFII Detector Technical Design Report, Fermilab-Pub-96/390-E
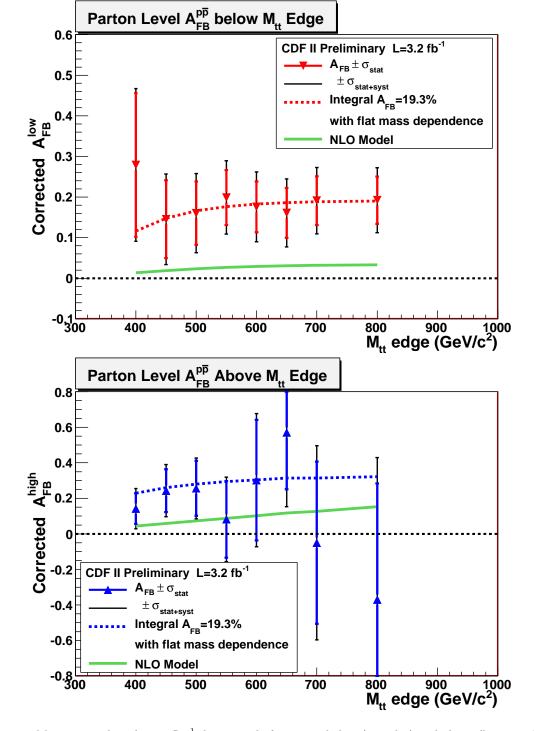
FIG. 6: A_{FB} vs $M_{t\bar{t}}$ measured in the 3.2 fb^{-1} data sample for events below (top plot) and above (bottom plot) the invariant mass edges shown by the x-axis. The data point with error bars are the central value returned by the two variable unfold; the inner error bars are the statistical uncertainties as returned by the unfold; the outer bars are the sum of the statistical and systematic uncertainties. The dashed line corresponds to a template of null $dA_{FB}/dM_{t\bar{t}}$ and A_{FB}^0 such to generate an integral $A_{FB} = 19.3\%$, as measured in the data. The green solid line shows the results for a model with $dA_{FB}/dM_{t\bar{t}} = 2.5\%$ and $A_{FB}^0 = 3\%$ as derived from the fit to the NLO calculation.

	Forward-Backward Asymmetry Below $M_{t\bar{t}}$ Threshold			
$M_{t\bar{t}}$ (GeV/c^2)	Raw $\mathcal{A}_{FB}$	Bkgr $\mathcal{A}_{FB}$	$\mathcal{A}_{FB}$ after bkg. sub.	Corr A_{FB}^{low} $\pm\sigma_{stat}\pm\sigma_{syst}$
400	0.111±0.057	-0.072±0.012	0.152±0.070	0.28±0.18±0.06
450	0.0755±0.043	-0.069±0.009	0.105±0.052	0.15±0.10±0.06
500	0.084±0.040	-0.060±0.009	0.112±0.048	0.16±0.08±0.06
550	0.099±0.038	-0.059±0.008	0.130±0.045	0.20±0.07±0.06
600	0.092±0.037	-0.059±0.008	0.122±0.044	0.18±0.06±0.06
650	0.087±0.036	-0.061±0.008	0.116±0.044	0.16±0.06±0.06
700	0.099±0.036	-0.059±0.008	0.130±0.043	0.19±0.06±0.06
800	0.100±0.036	-0.058±0.008	0.131±0.043	0.19±0.06±0.06

	Forward-Backward Asymmetry Above $M_{t\bar{t}}$ Threshold			
$M_{t\bar{t}}$ (GeV/c^2)	Raw $\mathcal{A}_{FB}$	Bkgr $\mathcal{A}_{FB}$	$\mathcal{A}_{FB}$ after bkg. sub.	Corr A_{FB}^{high} $\pm\sigma_{stat}\pm\sigma_{syst}$
400	0.089±0.046	-0.048±0.011	0.113±0.054	0.14±0.09±0.07
450	0.146±0.063	-0.031±0.015	0.176±0.074	0.24±0.12±0.08
500	0.16±0.08	-0.05±0.02	0.196±0.096	0.26±0.15±0.07
550	0.09±0.11	-0.050±0.027	0.11±0.13	0.08±0.22±0.10
600	0.20±0.16	-0.038±0.038	0.24±0.18	0.30±0.34±0.16
650	0.38±0.17	0.032±0.05	0.42±0.19	0.57±0.32±0.27
700	0.06±0.24	-0.008±0.072	0.066±0.267	-0.05±0.46±0.30
800	-0.14±0.38	-0.13±0.12	-0.14±0.40	-0.37±0.65±0.46

TABLE I: Summary of low and high mass region asymmetries for each $M_{t\bar{t}}$ edge considered in this analysis. The different columns report the calculated asymmetries at different stages in the unfolding procedure, namely for the raw number of events at reconstruction level (raw $\mathcal{A}_{FB}$), for the background events (bkgr $\mathcal{A}_{FB}$), for data events after background subtraction ($\mathcal{A}_{FB}$ after bkg. sub), and for the corrected number of events after the unfolding (corr A_{FB}). All uncertainties are statistical only, except for the corrected asymmetries value, for which both the statistical uncertainty returned by the unfolding, and the sum of the systematic uncertainties discussed in Section VI, are listed.

[2] The CDF Collaboration, http://www-cdf.fnal.gov/cdfnotes/cdf9724_ttbarAfbMeasurement.pdf, Mar. 2009

[3] J.H.Kuhn and G. Rodrigo, Phys. Rev. D59, 054017 (1999); M. T. Bowen, S. Ellis, and D. Rainwater, Phys. Rev. D 73, 014008 (2006)

[4] V.M. Abazov *et al.*, D0 Collaboration, Phys. Rev. Lett. 100, 142002 (2008).

[5] O. Antunano, J. H. Kuhn, G. Rodrigo, Phys. Rev. D 77, 014003 (2008); P. Ferrario and G. Rodrigo, arXiv:0809.3354 (2008);

[6] T. Aaltonen *et al.*, CDF Collaboration, Phys. Rev. D 77 051102 (2008).

[7] The CDF Collaboration, http://www-cdf.fnal.gov/cdfnotes/cdf9164_MG_DLM.pdf, Dec. 2007.

[8] T. Aaltonen *et al.*, CDF Collaboration, arXiv:0903.2850v1.pdf (2009).

[9] L. Almeida, G. Sterman, W. Vogelsang, "Threshold Resummation for Top Quark Change Asymmetry" arXiv:0805.1885v1/

[10] We use the symbols $\mathcal{A}_{FB}$ or y or $\mathcal{M}_{t\bar{t}}$ to indicate variables in reconstructed space and A_{FB} or Y or $M_{t\bar{t}}$ for variables in MC generated, or truth, space.